





MRI in patients with urethral stricture: a systematic review

Mikolaj Frankiewicz 
Karolina Markiet 
Jakub Krukowski 
Edyta Szurowska 
Marcin Matuszewski 

ABSTRACT

Magnetic resonance imaging (MRI) is gaining acceptance as a diagnostic tool in urethral stricture disease. Numerous publications emphasize on the advantages of MRI including its ability to determine periurethral spongiofibrosis, thus overcoming the main limitation of retrograde urethrography (RUG). It is also becoming an alternative for sonourethrography (SUG), which is a highly subjective examination. Magnetic resonance urethrography (MRU) has become an increasingly appreciated tool for diagnosing patients with urethral stricture disease. Obtained data provides radiologists and urethral reconstructive surgeons with additional information regarding anatomical relationships and periurethral tissue details, facilitating further treatment planning. Considering the great prevalence of urethral stricture disease and necessity of using accurate, and acceptable diagnostic method, this review was designed to provide radiologists and clinicians with a systematic review of the literature on the use of MRI in the urethral stricture disease.

Urethral stricture is one of the common male urological disorders with an increasing incidence. Patients may be asymptomatic or present with decreased urine flow, increased pressure required for urinating, a feeling of incomplete urination, urinating in a drop by drop manner and urinary retention. Moreover, ejaculation disorders, often underestimated by physicians, may be encountered, significantly influencing patients' quality of life (1).

Stricture might be caused by inflammatory, traumatic, ischemic, congenital or iatrogenic factors resulting in formation of scar tissue along the tract and reducing the caliber of the urethra (2). Disease is associated with high recurrence rate. Mechanisms underlying traumatic strictures include straddle injury, pelvic fracture-related urethral injury and iatrogenic injury secondary to instrumentation also in reference to worldwide increase in endoscopic transurethral treatment methods in the last decades (3).

Given that the number of patients suffering from urethral stricture disease is increasing, there is a need for improvement of diagnostic methods determining the choice of the optimal treatment method. Despite numerous surgical methods for treatment of this disease, it is still associated with high recurrence rates.

Process of stricture formation is usually associated with scarring within corpus spongiosum and is known as spongiofibrosis. Histological and immunohistochemical studies showed significant changes within the structure of the strictured part of urethral wall in the microscopic images. In contrast to normal urethra wall, the epithelial layer at the site of a stricture is much thicker. Collagen and bundles of elastin are densely packed around the strictured urethra (4). Thus, the most effective method of treatment for patients with urethral stricture with extensive spongiofibrosis is excision of the whole stricture followed by an end-to-end anastomosis of the two healthy ends (5). Therefore, more and more radiologists and urologists require information on the presence of spongiofibrosis and periurethral pathologies for the correct choice of treatment method.

Methods of urethral stricture evaluation

Urethroscopy

Despite the fact that urethroplasty has a much higher long-term success rate and better outcomes in terms of recurrence rate than dilatations and urethrotomies, minimally invasi-

From the Department of Urology (M.F. ✉ mfrankiewicz@gumed.edu.pl, J.K., M.M.), and Department of Radiology, (K.M., E.S.), Medical University of Gdansk, Gdansk, Poland.

Received 15 October 2019; revision requested 4 December 2020; last revision received 10 January 2020; accepted 17 February 2020.

Published online 19 November 2020.

DOI 10.5152/dir.2020.19515

You may cite this article as: Frankiewicz M, Markiet K, Krukowski J, Szurowska E, Matuszewski M. MRI in patients with urethral stricture: a systematic review. *Diagn Interv Radiol* 2021; 27: 134–146

ve methods are still most commonly used (6). Hence, urethroscopy is one of the most frequently performed diagnostic tools with the possibility of simultaneous treatment. However, urethroscopic evaluation may be limited or impossible depending on the degree of the stricture. Its main limitation is revealed when diagnosing patients with a significant or complete stricture. In such cases the introduction of the tool is often impossible which makes the evaluation of stricture length, number, and location impossible, especially when multiple strictures are present. This limitation, in some cases, may be overcome by using instruments with a smaller diameter (e.g., pediatric cystoscope, or flexible urethroscope) (7). As indicated by some authors, the possibility of assessing the extent of the scar on the basis of color and macroscopic view is not reliable as it concerns only the superficial layer. In some cases, antegrade cystoscopy may show some value, because it allows assessment of the bladder neck, sometimes enables evaluating the mobility of the sphincter and identification of the urethral lumen in severe strictures.

Urethrography

Retrograde urethrography (RUG) and voiding cystourethrography (VCUG) are still the most commonly used diagnostic tools. In order to visualize the urethral lumen, iodinated contrast is introduced into the urethra under fluoroscopic view. The main

advantage of this tool is that it instantly diagnoses the location, number and length of the strictures. It does not however, provide assessment of pathologies that extend beyond the urethral lumen. RUG usually also enables diagnosis of urethral wall damage, fistula or false passage (8). Yet, the importance of urologists' involvement in both performing and interpretation of urethrography should be emphasized. Bach and Rourke reported that preoperative assessment of the stricture located in anterior urethra is adequate in only 87% of cases when evaluated by the radiologist, compared with 96% when read by a urologist. Moreover, only 49% of the reports generated by a radiologist are adequate for interpretation (9). Sometimes administration of contrast is painful, or leads to extravasation to the corpora cavernosa, or veins. Special care must be taken not to misdiagnose it as additional pathologies, e.g., a false path. In cases in which the stricture is close to the external meatus, it is difficult to perform the examination because the insertion of the catheter is frequently impossible. Another limitation is that despite performing the examination at an angle of 45 degrees, the spatial localization of the stricture cannot be assessed, therefore it is difficult to measure its length. Considering the safety of both the patient and the physician, these procedures carry a significant radiation exposure. In case of standard diagnostics, the amount of radiation does not pose a major threat, but it may become a problem for patients requiring numerous re-examinations especially those of young age (10). What is important, the irradiated region concerns the gonads, that are particularly vulnerable to the adverse effects of radiation.

Sonourethrography

Until recently, identifying the healthy corpus spongiosum intraoperatively could be done by visual macroscopic assessment. One of the alternative methods used to diagnose and assess urethral strictures is sonourethrography (SUG). Sonourethrography allows assessment of the bulbar urethra stricture length more accurately than RUG and detects periurethral spongiosclerosis (11, 12). Compared to VCUG, SUG demonstrates higher accuracy for strictures arising from traumatic catheterizations and idiopathic stenoses. Lower accuracy was observed in evaluation of posttraumatic strictures which are usually located in the bulbar urethra, often difficult or impossible

to be depicted by SUG, especially in obese patients. Technique is straightforward, readily available and cost effective. The biggest limitation is the high subjectivity of the study. It is relatively easy to over-diagnose a urethral stricture if the ultrasound probe is used with too much pressure on the urethra during the test. Moreover, the assessment of multiple or long strictures is limited because of small field-of-view (13).

Magnetic resonance urethrography

In recent years, numerous publications focused on magnetic resonance urethrography (MRU) which enables pre-operative assessment of urethral stricture, providing information about the degree of spongiosclerosis. It provides excellent soft tissue contrast, and depicts the urethra and periurethral structures without exposure to radiation. MRU is also reported to show particular effectiveness in diagnosing strictures that occur after pelvic injuries, providing additional information about the prostatic apex displacement. MRU may also give information on the cause of posttraumatic impotence as some authors describe the relation between avulsion of the corpus cavernosum and the potency (14, 15).

Considering the growing incidence of urethral stricture and the necessity of using an accurate and acceptable diagnostic method, this paper was designed to give clinicians a systematic review of the literature on the use of magnetic resonance in the urethral stricture disease. Anatomy and pathology will be described, with an emphasis on the optimal imaging protocol and considerations. In the available literature, there are few conclusive data on indications, advantages and limitations of the MRU. The analysis aims to include optimal data on these aspects and provide the clinician with an answer on when and how to use MRU.

Data acquisition

Comprehensive literature search without a time limit was performed by two independent researchers using PubMed and Scopus - Internet-based bibliographic databases with limitation to articles published in English, Polish or French. The authors followed the Preferred Reporting Items for Systematic Reviews and Meta-Analysis (PRISMA) statement. The process of selection of articles is presented in the PRISMA flowchart (Fig. 1) (16, 17). Studies that examined the use of magnetic resonance imaging (MRI) in

Main points

- As the number of patients suffering from urethral stricture disease is increasing, there is need for improvement of diagnostic methods to help choose the optimal treatment method.
- MRI provides excellent soft tissue contrast and adds extra information compared with conventional methods by depicting the urethra and periurethral tissues with the advantage of avoiding radiation.
- The role of MRI in evaluation of the urethral strictures is significant, providing the surgeons with crucial data that influences treatment planning; yet, the greatest usefulness of MRI is demonstrated in post-traumatic urethral strictures, multiple strictures and long strictures with extensive spongiosclerosis.
- Further studies on more numerous groups of patients suffering from urethral stricture disease should be designed and correlated with clinical outcomes in order to provide sufficient data on MRI indications and technique.

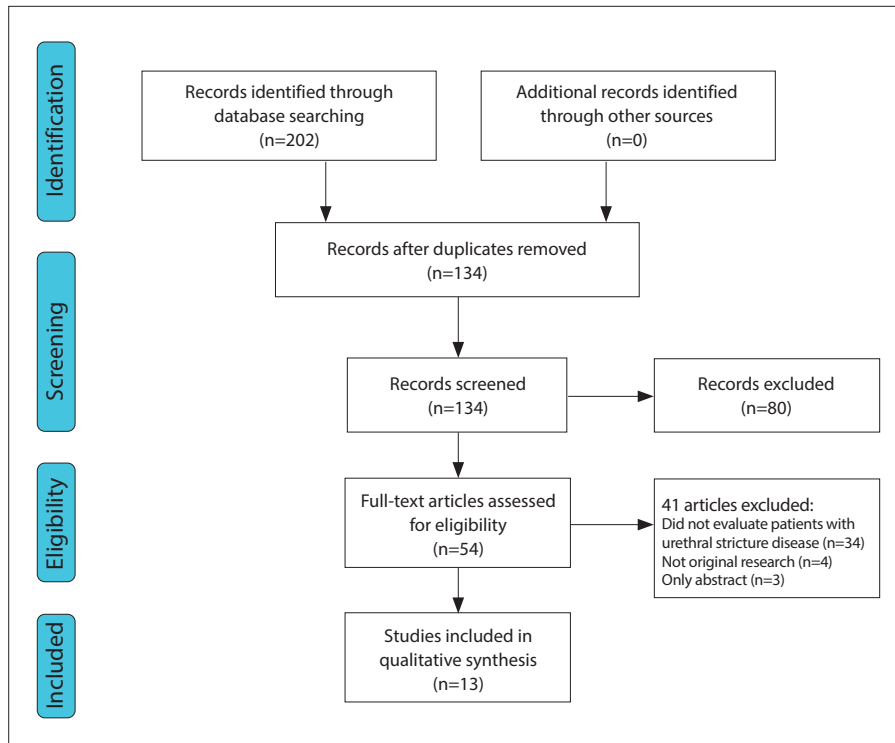


Figure 1. PRISMA flowchart.

the diagnosis of urethral stricture disease were selected. The following search criteria were entered into the 2 databases in March 2019: (“MR” OR “MRI” OR “MRU” OR “magnetic resonance”) AND (“urethroplasty” OR “urethral stricture” OR “urethral stenosis” OR “urethral injury” OR “urethral surgery” OR “urethral reconstruction” OR “pelvic fracture”). There was no restriction in years of publication. Overall, 70 abstracts were found by PubMed, and 202 using the Scopus database. In total 272 abstracts were selected for analysis and 68 duplicates were rejected from further consideration. Due to the diversity of the studies a qualitative analysis was performed.

Screening

Abstract screening was performed by the two researchers. Results of the screening were compared and differences were resolved by discussion.

The inclusion criteria were as follows: male patients with anterior or posterior urethral stricture, application of MRI in diagnosis of urethral stricture disease, articles published in English, Polish or French. The exclusion criteria were as follows: articles on female urethra, animal studies, abstracts of conferences, and editorials.

Thirteen articles fulfilled all the screening criteria and were selected for a qualitative

analysis. In total, these studies analyzed a population of 259 patients, aged 4–90 years.

Data analysis

Anatomy of male urethra

Male urethra measures approximately 17.5–20 cm and courses from the bladder to the external urethral meatus. It is divided into posterior and anterior parts.

Posterior urethra extends from the neck of the bladder to the inferior rim of the urogenital diaphragm and consists of prostatic and membranous segments. Prostatic urethra is approximately 3.5 cm in length and runs through the central part of posterior prostate gland as seen in the axial plane. Urethral crest, a longitudinal ridge of smooth muscle, is seen on the posterior wall from the bladder neck to the membranous urethra and continues into the verumontanum. Prostatic utricle lies in the center of the verumontanum with the orifices of ejaculatory ducts just distal and lateral to it. Membranous urethra is approximately 10 mm long and traverses the urogenital diaphragm. Internal urethral sphincter extends from the bladder neck through the prostatic urethra above the verumontanum. The urogenital diaphragm is seen on axial T2-weighted images as a hypointense ring surrounding the hyperintense epithe-

lial surface (18). It contains the external urethral sphincter and a Cowper gland on each side of the membranous segment of the urethra. Measuring approximately 2 cm in length, the ducts of Cowper glands empty into the bulbar urethral sump (19).

Anterior urethra runs through the corpus spongiosum from the inferior edge of urogenital diaphragm to the external meatus. It consists of bulbar and penile (or pendulous) segments. Penile urethra extends from the penoscrotal junction to the external meatus and terminates in the glans penis to form the fossa navicularis. Bulbar urethra lies between the inferior margin of the urogenital diaphragm and the penoscrotal junction. Proximal, dilated part of the bulbar urethra is called the sump. Just proximally to the sump, at the bulbomembranous junction, the shape of the urethra is conical (the cone). Anterior urethra contains periurethral Littre glands with the majority at the dorsal outline of penile urethra and at the sump. Proximal portion of prostatic urethra and distal part of penile urethra are often not seen on MRI unless a Foley catheter is placed (20). Fig. 2 presents selected features from the anatomy of male urethra.

MRI protocol and considerations

Imaging protocols as well as applied sequences differ between published studies. Optimal visualization of the male urethra requires proper positioning and preparation of the patient. Patient lies in supine position. Some authors advise to elevate the penis and the scrotum by placing a towel between these structures and the upper thighs (21). The examination is performed with the penis in a flaccid state. A catheter with attached syringe filled with 10–20 mL of sterile lubricating anesthetic gel is introduced into the urethral meatus and gel is infused to distend the urethra sufficiently (22, 23). Some authors report usage of saline solution (24, 25); however, the risk of spillage is increased with the latter, especially in the presence of associated fistula. This technique ensures high-contrast resolution with good visualization of the tunica albuginea and facilitates evaluation of urethral pathologies including stricture (26). Glans sulcus is tied using gauze to prevent leakage of the gel and the dorsiflexed penis is secured (taped) against the anterior wall of the abdomen in the midline; penis should not be rotated along its long axis (27). Table 1 presents detailed description

of modifications and methods of patient preparation before MRU.

Examination is usually performed with a body coil. At some institutions surface coils are used when imaging the posterior urethra, while anterior urethra is studied with a phased-array pelvic and/or body coil (28). According to some authors, endocavitary coils improve spatial resolution; however, small field of view may limit imaging area and high signal intensity in the near field decreases image quality (18). Application of a 3 T high-field MRI unit with multi-channel phased-array coils leads to higher image quality (26). Thin section thickness (3–5 mm) and small intersection gap (1–2 mm) are required (18). Routinely both

T1- and T2-weighted sequences are obtained. All authors underline the importance of high-resolution T2-weighted imaging. Generally axial and coronal images prove to be more useful in the evaluation of the posterior urethra, while sagittal images are dedicated to assessment of the anterior urethra (26). Urethra is isointense to muscle on T1-weighted imaging, while the tunica albuginea and spongiosum tissue are hyperintense. The verumontanum is hyperintense in T2-weighted imaging sequences. Distal prostatic urethra has an additional muscle layer, which demonstrates low signal on T2-weighted imaging. Membranous urethra shows low signal on T2-weighted imaging referring to fibers of the external sphincter.

Multiplanar images are obtained to outline the entire length of the urethra, define the surrounding soft tissues with focus on depth and density of periurethral fibrosis, and determine stricture length if present (25). Total stricture length is measured with inclusion of tapered segments on either side of the tight stricture (28–30). Spongiofibrosis is depicted on T1- and T2-weighted images as hypointense areas distinguishable from normal spongy tissue (23).

Contrast-enhanced MRI may be profitable in cases of extensive tumors and inflammation involving the urethra and periurethral tissues (18). It allows precise delineation of the actual site, extension, and activity of the inflammatory process (Fig. 3). In patients with pelvic trauma, dislocated bone fragments may also be depicted (28). Post-gadolinium imaging is advised to be performed with a fat-suppressed isotropic sequence to allow multiplanar reconstructions. To obtain contrast-enhanced sequences, a gadolinium contrast agent is routinely used at the standard dose of 0.1 mmol/kg of body weight (0.1 mL/kg of body weight) at a rate of 2 to 3 mL, followed by a 20 mL saline flush. General considerations and contraindications apply to both MRI and gadolinium-based contrast agents (31).

Some authors propose performing contrast-enhanced 3D magnetic resonance voiding urethrography. After intravenous injection gadolinium-based contrast agent, images are obtained during voiding. According to Yekeler et al. (32) the excretory

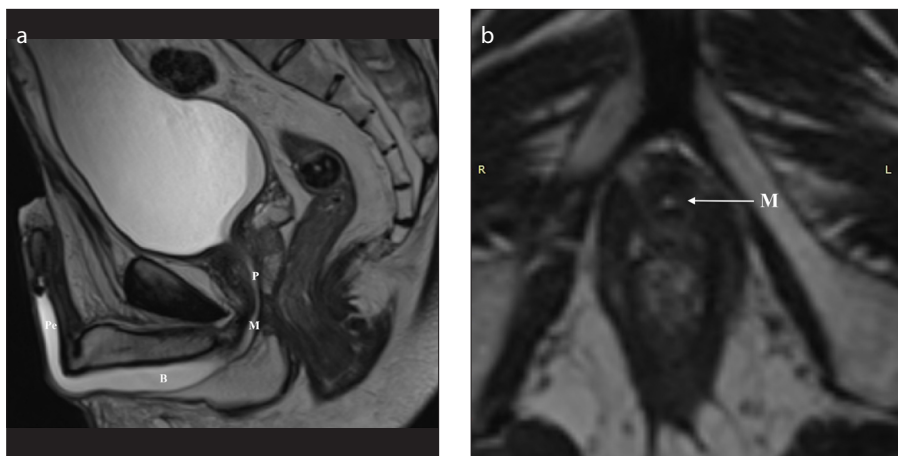


Figure 2. a, b. Imaging anatomy of the male urethra in a 35-year-old man. T2-weighted sagittal image (a) after distention of the urethra with sterile gel shows the prostatic urethra (P), level of the membranous urethra (M), and both bulbar (B) and penile (P) parts of the anterior urethra. T2-weighted axial image (b) at the level of the genitourinary membrane shows urethra as a small round structure of high signal intensity (arrow).

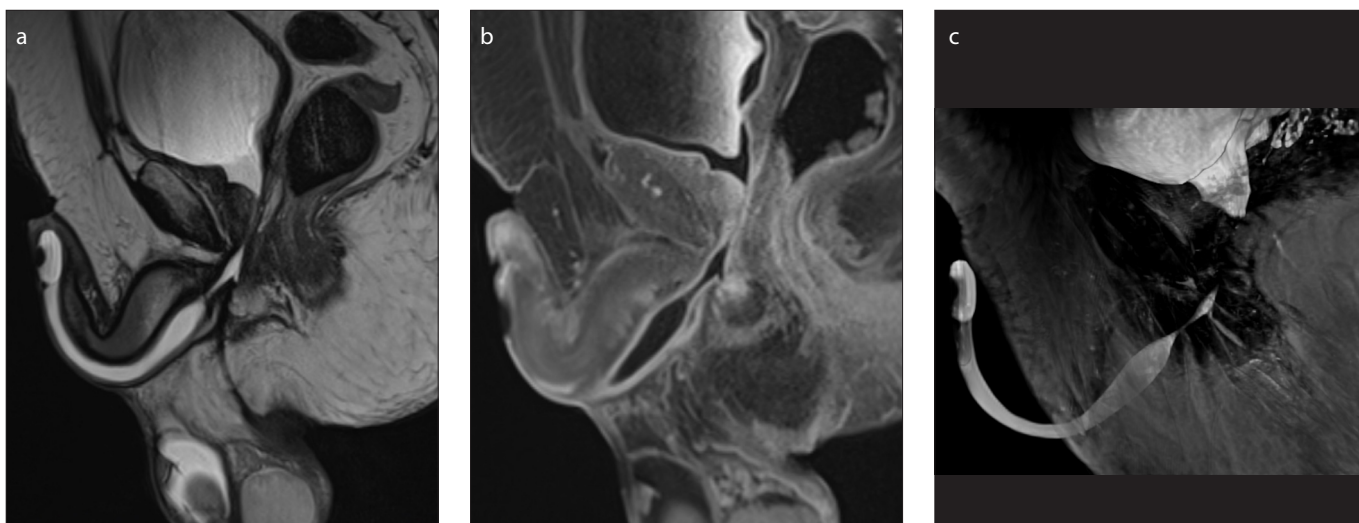


Figure 3. a–c. A 72-year-old patient who developed an urethral stricture due to straddle injury followed by multiple interventions, currently after removal of chronic Foley catheter. Status post transurethral resection of the prostate (TURP). T2-weighted sagittal image (a) shows a 24.5 mm stricture of the bulbar urethra—the site and extension of the stenosis are well depicted by the distended urethra. After intravenous administration of contrast agent, the activity of the inflammatory process can be evaluated (b). MIP reconstruction is also enclosed (c).

Table 1. Modifications and methods of MRU for diagnosing urethral stricture disease

Study	n	Age (y)	Techniques	Location	Cause of the stricture	MRI unit	Exam protocol	Points of evaluation	Reference	Mean stricture length	Aim of the study	Results/Additional remarks
Dixon et al. 1992	18	4-71	MRI	Posterior	Trauma	1.5T (n=11) 0.35T (n=5)	11 examinations: 1. Tra T1WI (TR/TE 500 / 20 ms) 2. Tra Sag Cor T2WI (TR /TE 2500 / 70-80 ms) 3. Tra Sag Cor PD (TR /TE 2500 / 30 ms; section thickness 4 mm, matrix 192x 256) 5 examinations: 1. Tra T1WI (TR/TE 500 / 30 ms) 2. Tra Sag Cor T2WI (2000 / 60 ms; slice thickness 5 mm, matrix 256x256)	Length of injury; Displacement of prostate in 3 planes; Pelvic bone fracture	Surgery	No data	To examine the role of MRI in post-traumatic pelvic anatomy Optimizing surgical treatment	MRI can determine the length of urethral defect and severity of prostatourethral dislocation
Narumi et al. 1993	27 (+1 HC)	4-71	MRI	Posterior	Trauma	1.5T (n=23) 0.35T (n=5)	23 examinations (22 patients, 1 HC): 1. Tra T1WI (TR/TE 500 / 20 ms) 2. Tra Sag Cor T2WI (2500 / 70-80 ms) 3. Tra Sag Cor PD (2500 / 30 ms; section thickness 4 mm, matrix 192x 256) 4. 3 patients - T2WI FSE (3800- 4500 / 96-106 ms; slice thickness 4 mm, matrix 512x 256) 5 examinations: 1. Tra T1WI (TR/TE, 500 / 30 ms) 2. Tra Sag Cor T2WI (2000 / 60 ms; slice thickness 5 mm, matrix 256x 256)	Length of injury; Displacement of prostate in 3 planes; Presence and type of penile injury; Pelvic bone fracture	Surgery	No data	To examine the role of MRI in preoperative evaluation of posterior urethral injury; To evaluate the role of MRI in predicting permanent erectile dysfunction after posterior urethral injury	Length of the injury measured correctly in 85% cases. Displacement of the prostate apex in 90% patients. MRI findings caused alteration in surgical procedure in 7 (26%) patients
Yekeler et al. 2004	18 (12 with strictures, 5 healthy controls)	43.3 (22-90)	3D MRVU vs. RUG (n=10) and urethroscopy (n=12)	Anterior (n=7), posterior (n=7)	Urinary bladder cancer (n=1), Prostatic hypertrophy (n=5), Unknown (n=12)	1.5T	1. Cor and HASTE (TR /TE, 1/82 ms; matrix, 75x 256; FOV 300x 180 mm; slice thickness, 6 mm; gap, 0.6 mm) 2. Sag T1WI 3D FLASH (3.2/1.1 ms; flip angle, 308; slab thickness, 94-112 mm; slice thickness, 1 mm; FOV, 300x 180 mm; matrix, 300-320x 512; acquisition time, 35 s) 3. Cor T1WI 3D FLASH (3.2/1.1 ms; flip angle, 308; slab thickness, 72 mm; slice thickness, 1 mm; FOV, 300x 180 mm; matrix, 300-320x 512; acquisition time, 24 s)*	Stricture number and length	Urethroscopy; 5 healthy volunteers for anatomy outline	[cm] RUG: 2.4 (0.7-3.2) MRI: 2.1 (0.5-3.1)	To assess the feasibility of CE MRVU with the use of the CE 3D MRA technique in healthy volunteers and in patients with urethral strictures	Severe membranous urethral strictures better demonstrated by CE 3D MRVU. CE 3D MRVU superior to RUG in demonstration of normal urethra in the proximal junction of strictures in patients with membranous and bulbous urethral strictures

Table 1. Modifications and methods of MRU for diagnosing urethral stricture disease (cont'd)

Study	n	Age (y)	Techniques	Location	Cause of the stricture	MRI unit	Exam protocol	Points of evaluation	Reference	Mean stricture length	Aim of the study	Results/Additional remarks
							<ol style="list-style-type: none"> MRVU Sag T1WI 3D FLASH (3.2/1.1 ms; flip angle, 308; slab thickness, 44 mm; slice thickness, 1 mm; FOV 300×80 mm; matrix 300–320×512; acquisition time, 15 s). 3 consecutive acquisitions (0, 15 and 30 s) and to evaluate bladder residual volume. 4-element phased-array body coil *6-channel phased-array spine coil Voiding before MRI 0.3 mL/kg Gd-DTPA prior to CE 3D MRVU Readiness to urinate 55–170 min (mean, 70 min) post i.v. contrast injection 					
Osman et al. 2006	20	55±19 (17-77)	MRI vs. RUG+VCUG	Anterior and posterior	Postinflammatory (n=16), Iatrogenic injury (n=2), Trauma (n=2)	No data	<ol style="list-style-type: none"> Sag high-resolution T2WI (TR/TE 4000–6000/80–120 ms, slice thickness 2 mm, gap 0 mm). Reformatted images at axial, coronal, and sagittal oblique planes Sterile gel 	Entire urethra; Surrounding soft tissues; Periurethral fibrosis; Stricture length	Urethroscopy followed by definitive endoscopic or open operative intervention	[cm] RUG +VCUG: 1.5±1.3 MRI: 1.2±0.9	To compare clinical relevance of RUG~ and MRU in male urethral strictures	MRI findings caused alteration on surgical procedure in at least 4 patients. No difference in stricture length between the modalities ($p = 0.25$). Same accuracy for diagnosis of urethral strictures (85%). MRU provided extra clinical data in 7 patients (35%). MRU superior to RUG in evaluating surrounding tissues. MRU provided adequate information about the degree of spongiobrosis in all patients.

Table 1. Modifications and methods of MRU for diagnosing urethral stricture disease (cont'd)

Study	n	Age (y)	Techniques	Location	Cause of the stricture	MRI unit	Exam protocol	Points of evaluation	Reference	Mean stricture length	Aim of the study	Results/Additional remarks
Sung et al. 2006	12	48.4 (21-83)	MRI vs. RUG+VCUG	Anterior and posterior	Radical prostatectomy (n=1). Trauma (n=11)	1.5T	<ol style="list-style-type: none"> 1. Sag T2WI FSE (TR/TE 3000/99 ms) 2. Tra T2WI FSE (3200/99 ms; FOV, 24 cm; matrix, 512x 264; section thickness 3 mm; gap 0.1 mm) 3. Sag T2WI FSE (3000/99 ms) 4. Tra T2WI FSE (3200/99 ms; FOV 24 cm; matrix, 512x 264; section thickness 3 mm; gap 0.1 mm) 5. Sag T1WI SE (473/20 ms) 6. Sag T1WI SE (473/20 ms) post 0.1 mmol/kg Gd-DTPA (3 min) <ul style="list-style-type: none"> • Pelvic phased-array coil • Distention of urethra with saline 	Signal intensity, location, length, and contrast enhancement of the stricture; Urethra proximal to the stricture; Corpora spongiosa; Adjacent organ injuries	Surgical specimen or a report on surgical findings	No data	To evaluate MRU for the depiction of obliterative urethral strictures; To compare the accuracy of MRU versus VCUG in estimating the length of obliterative urethral stricture	MRI findings caused the change in surgical procedure in 7 of the 10 patients. Stricture length overestimated in 58% patients in MR and 60% in RUG + VCUG. Mean measurement error at MRI significantly lower than in RUG + VCUG. Stronger linear relationship between MRI and surgical measurements
Koraitim et al. 2007	21	6-35	MRI vs. RUG+VCUG	Posterior	Trauma	0.2T	<ol style="list-style-type: none"> 1. Tra Sag T1WI FSE (TR/TE 690/15 ms; slice thickness 5 mm) 2. Tra Sag T2WI FSE (3400-4000/ 106 ms; slice thickness 4 mm) 3. Sag T2WI FSE with fat suppression (3400-4000/ 106 ms; slice thickness 4 mm) 4. Cor T2WI FSE (3400-4000/ 106 ms; slice thickness 4 mm) 	Urethral distraction; Associated injuries	Surgery	No data	To determine clinical usefulness of MRI in assessment of posterior urethral distraction defects; To determine if MRI can identify the cause of posttraumatic impotence	Length of urethral defect and type of prostatic displacement could be correctly determined in MRI in 86% and 89% of the patients, respectively
El-ghar et al. 2010	30	45±18 (15-75)	MRI vs. RUG+SUG	Anterior and posterior	No data	No data	<ol style="list-style-type: none"> 1. Sag high-resolution T2WI (TR/TE 4000–6000/80–120 ms, slice thickness 2 mm, gap 0 mm) 2. Reformatted images at axial, coronal, and sagittal oblique planes <ul style="list-style-type: none"> • Sterile gel 	Stricture length; Associated pathology; Abnormal communication	Surgery	[mm] RUG: 13.3±5.7 (3-24) SUG: 11.2±4.9 (3-20) MRI: 11.4 (3-20) Surgery: 11.3 (3-20)	To compare the accuracy of MRU versus combined RUG and SUG in diagnosis of urethral stricture with evaluation of their impact on management choice	MRU comparable with RUG+SUG in diagnosing the anterior and posterior urethral strictures regarding the site and extension and degree of spongiofibrosis but MRU is superior in diagnosis of associated pathologies with stricture

Table 1. Modifications and methods of MRU for diagnosing urethral stricture disease (cont'd)

Study	n	Age (y)	Techniques	Location	Cause of the stricture	MRI unit	Exam protocol	Points of evaluation	Reference	Mean stricture length	Aim of the study	Results/Additional remarks
Oh et al. 2010	25	48.7 (21-72)	MRI vs. RUG+VCUG	Posterior	Trauma (n=24), Radical prostatectomy (n=1)	1.5T	<ol style="list-style-type: none"> Sag T2WI FSE (TR/TE 3000/99) Tra T2WI FSE (3200/99, FOV 24 cm, matrix 512x264, slice thickness 3 mm, gap 0.1 mm) Sag T1WI SE (473/20) Sag T1WI SE post 0.1 mmol/kg Gd-DTPA (3 min delay) <ul style="list-style-type: none"> Pelvic phased-array coil Sterile gel Emptied bladder filled with 200-300 mL saline through the suprapubic catheter until need to void 	Stricture length	Surgery	[cm] RUG + VCUG (n=22): 2.3 MRI: 1.56 Surgery: 1.51	To evaluate the role of MRU in depicting obliterative urethral stricture	Mean SD measurement error in MRU significantly less than that RUG + VCUG (0.4±0.4 vs. 1.4±1.1 cm, <i>p</i> < 0.001). Stronger linear relationship between MRU and surgical measurements (<i>r</i> ² =0.62, <i>p</i> < 0.01).
Park et al. 2010	10	61.7 (47-77)	SSFSE MRU vs. FRFSE MRU vs. RUG	Anterior	TURP (n=4), Laser surgery of the prostate (n=2), Trauma (n=4)	1.5T	<ol style="list-style-type: none"> Sag T2WI TS-SSFSE (TR/TE 4595-4699/176 ms, slice thickness 20 mm, gap 0 mm, matrix 512x448) Sag T2WI FRFSE (TR 2900-3367 ms/TE 100 ms; slice thickness 3 mm, gap 0 mm, matrix 512x256) <ul style="list-style-type: none"> Sterile gel 	Location, type, length and internal diameter of the stricture; MRI image quality	MRU	[mm] MRI: 1. TS-SSFSE 36.4± 21.8 (4.0- 71.3) 2. FRFSE 35.7± 20.8 (4.0- 67.5) Surgery (n=8): 18.8± 4.8 (15-25) Internal diameter: 1. TS-SSFSE 0.73± 0.80 (0-1.8) mm 2. FRFSE 0.77± 0.74 (0-2.1) mm	To determine the role of TS-SSFSE vs. FRFSE for evaluating anterior urethral stricture	TSSSFSE MRU can provide useful information on anterior urethral strictures; it allows obtaining a RUG-like image during an ultra-short scan time. TSSSFSE MRU may not be sensitive enough to detect sophisticated periurethral changes due to inferior image quality
Khalaf et al. 2015	20	49.6± 16.4 (19-70)	MRI vs. RUG	Anterior	No data	1.0T	<ol style="list-style-type: none"> Sag T1WI FSE (TR/TE 400/20) Sag T2WI FSE (3000/99) Tra T2WI FSE (3200/99 ms; FOV 24 cm; matrix 512x264; thickness 3 mm; gap 0.1 mm) <ul style="list-style-type: none"> Pelvic phased-array coil Sterile gel 	Signal intensity, location and length of the stricture; Urethra proximal to the stricture; Corpora spongiosa; Adjacent organ injuries; Associated complications	Surgery	[cm] RUG: 1.75± 1.02/ MRI: 1.32± 0.85 Surgery: 1.29± 0.83	To evaluate diagnostic capability of MRU vs. conventional RUG in anterior urethral stricture	Accuracy of MRU 95%

Table 1. Modifications and methods of MRU for diagnosing urethral stricture disease (cont'd)

Study	n	Age (y)	Techniques	Location	Cause of the stricture	MRI unit	Exam protocol	Points of evaluation	Reference	Mean stricture length	Aim of the study	Results/Additional remarks
Hanna et al. 2015	18	37.37 (13-61)	MRI vs. RUG	Anterior and posterior	Trauma (n=13), Congenital (n=3), Post-inflammatory (n=2)	1.5T	1. Sag T2WI TSFSE (TR 4500-4700 ms, TE 176 ms, thickness 20 mm, gap 0 mm) 2. Sag T2WI FRFSE (TR 2900-3300 ms, TE 100 ms, thickness 3 mm, gap 0 mm) • Reformatted images at different planes • Pelvic phased-array coil • Sterile gel 16 pts • Sterile water 2 pts	Stricture length; Associated pathology	No data	No data	To evaluate utility of MRU vs. conventional urethrography in diagnosis and characterization of different urethral lesions	MRU superior in delineation and characterization of the urethral pathology in four cases (22.2%), diagnosing prostatic displacement as well as periurethral fibrosis, inferior in diagnosing a case of diffuse pseudodiverticulosis
Rastogi et al. 2016	20	18-72	MRI vs. SUG	N/A	Postinflammatory (n=10), Trauma (n=3), Iatrogenic (n=3), Idiopathic (n=1), Excluded (n=3)	1.5T	No data on exam protocol • Sterile gel	No data	No data	No data	To evaluate the comparative role of SUG and MRU in the evaluation of male anterior urethral strictures	MRU findings caused alteration in surgical procedure in 1 patient
Pandian et al. 2017	20	34 (17-61)	MRI vs. RUG+VCUG	Posterior	Trauma	3.0T	1. Tra Sag Cor T2WI 2. STIR_Long TR/RA, SS-TSE, SPAIR, SENSE. TR 3500ms/TE 90 ms; slice thickness 3 mm • Sterile gel	Urethral distraction; Associated injuries	Surgery	No data	To establish if MRI provides additional information for preoperative planning. To assess the role of MRI in counseling and management of PFUDD.	MRI provides detailed 3D images of urethral distraction defect

All studies were prospective except for Rastogi et al., in which the design was not specified.

Patients with multiple strictures were clearly identified only in Yekeler et al. (14 strictures in 12 patients).

Osman et al., El Gahr et al., and Khalaf et al. defined short stricture as <1.5 cm, long stricture as >1.5 cm. Park et al. defined short stricture as <2.5 cm, long stricture as >2.5 cm. Sung et al. defined short stricture as <1.0 cm, intermediate stricture as 1.0-2.5 cm, long stricture as >2.5 cm.

MRI, magnetic resonance imaging; Tra, transverse; T1WI, T1-weighted image; TR, time of repetition; TE, time of echo; Sag, sagittal; Cor, coronal; PD, proton density; MRU, magnetic resonance voiding urethrography; RUG, retrograde urethrography; TSE, turbo spin-echo; FOV, field of view; 3D, three dimensional; Gd-DTPA, gadopentate dimeglumine; CE, contrast enhanced; i.v., intravenous; VCUG, voiding cystourethrography; SUG, sonourethrography; TURP, transurethral resection of prostate; FSE, fast spin-echo; SSFSE, thick slab single-shot fast spin echo; FRFSE, fast recovery fast spin echo; STIR, short T1 inversion recovery; SPAIR, SPectral Attenuated Inversion Recovery, SENSE, SENSitivity Encoding; HASTE, half-fourier single shot turbo spin-echo; TS-SSFSE, thick slab single-shot fast spin-echo; SS-TSE, single-shot turbo spin-echo; PFUDD, posterior pelvic fracture urethral distraction defect.

phase is beneficial in revealing intraluminal and intracavitary urinary tract pathologies. Major limitations of MRU include availability, higher cost and longer learning curve for radiologists. Some authors suggest that restriction of MRU to patients with severe strictures would be more beneficial and prove cost-effective (30).

A variety of cases presenting strictures as well as complications and alterations within adjacent soft tissues are shown in Figs. 4–8.

MRI vs. other imaging methods

MRI in assessment of anterior urethral strictures:

Only few papers describe the use of MRI in patients with anterior urethral strictures. While inter-institutional variability is visible, application of T2-weighted imaging and proper positioning of the patient are emphasized. Sung et al. (33), reported that anterior and proximal portions of posterior urethra are rarely depicted on MRI. Osman et al. (30) showed that MRU diagnosed all

cases of both anterior and posterior strictures with 100% sensitivity, 91.7% specificity and 95% overall accuracy with precise assessment of length, but one case of a normal urethra falsely diagnosed as an anterior short-segment stricture. In another paper they compared RUG and MRI in 20 patients with urethral strictures, 18 of which anterior (22). The accuracy did not differ between the two methods, however MRI provided information about degree of spongiofibrosis, which according to the authors may

be helpful in choosing the treatment (8, 30). Rastogi et al. (34) compared the role of SUG and MRU in anterior urethral strictures. Detection rates of long-segment strictures differed significantly between these two methods. MRU detected the stricture properly in 82.4% of patients compared to only 58.8% by SUG in a group of 17 patients. The

misdiagnosis using SUG was associated with inaccurate classification of long strictures as short in 4 cases. Moreover, SUG failed to detect concomitant strictures located in the posterior part of urethra in 3 cases, all of which were properly detected by MRU. Based on the results of MRU, the authors decided on an open surgery in all 17 pa-

tients. Guided by the results of SUG, authors would have performed an open surgery in 16 patients, having misdiagnosed one case with a long-segment stricture with extensive spongiofibrosis in the posterior urethra.

MRI in assessment of posterior urethral strictures:

Both diagnosis and treatment of posterior urethral strictures are challenging. Urethral trauma causing stricture in males is usually a result of pelvic fracture, straddle and/or penetrating injury. Proper preoperative assessment of the extent of scar tissue, length and location of the stricture in relation to the sphincter is decisive. Moreover, information about prostatic apex displacement and assessment of the urethra axis may be crucial for choice of an optical surgical access. Although pelvic fracture typically results in the posterior urethra injury, with concomitant straddle trauma, the injury can include bulbar urethra, which alters treatment. Oh et al. (35) prospectively evaluated 25 men with complete posterior stricture. The authors showed that MRU was significantly more accurate in measuring the length of the stricture than RUG and VCUG combined. Hanna et al. (25) prospectively evaluated 18 male patients in order to verify the utility of MRU in diagnosis of different urethral lesions. The authors compared MRU with VCUG. In four cases (22.2%) MRU was superior in detection and characterization of urethral pathology. Three of the cases concerned posterior urethral strictures, two of which had prostatic displacement detected by MRU only. Osman et al. (30) compared clinical relevance of RUG and MRU by evaluating 20 patients with urethral strictures.

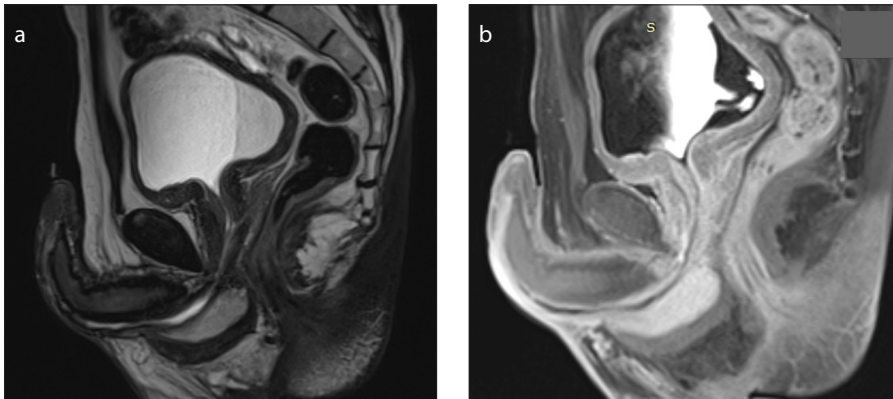


Figure 4. a, b. T2-weighted (a) and contrast-enhanced T1-weighted (b) sagittal images show long stenosis of the bulbar and penile segments in a 39-year-old patient.

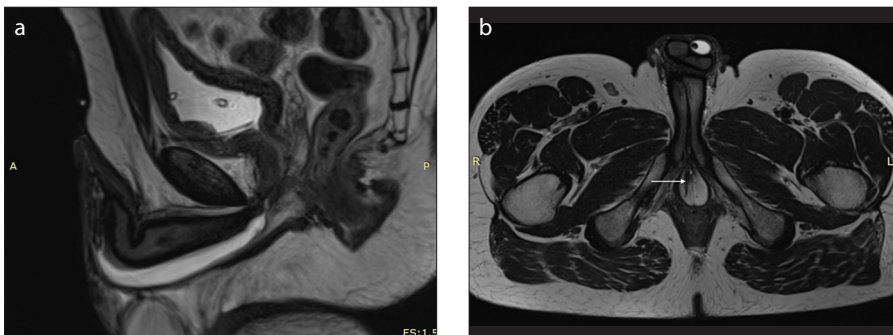


Figure 5. a, b. A 35-year-old patient with post-traumatic urethral stenosis. T2-weighted sagittal image (a) shows severe stenosis of the bulbar urethra and axial image (b) shows a fistula in the right penile bulb (arrow). The fistula was limited to the right penile bulb.

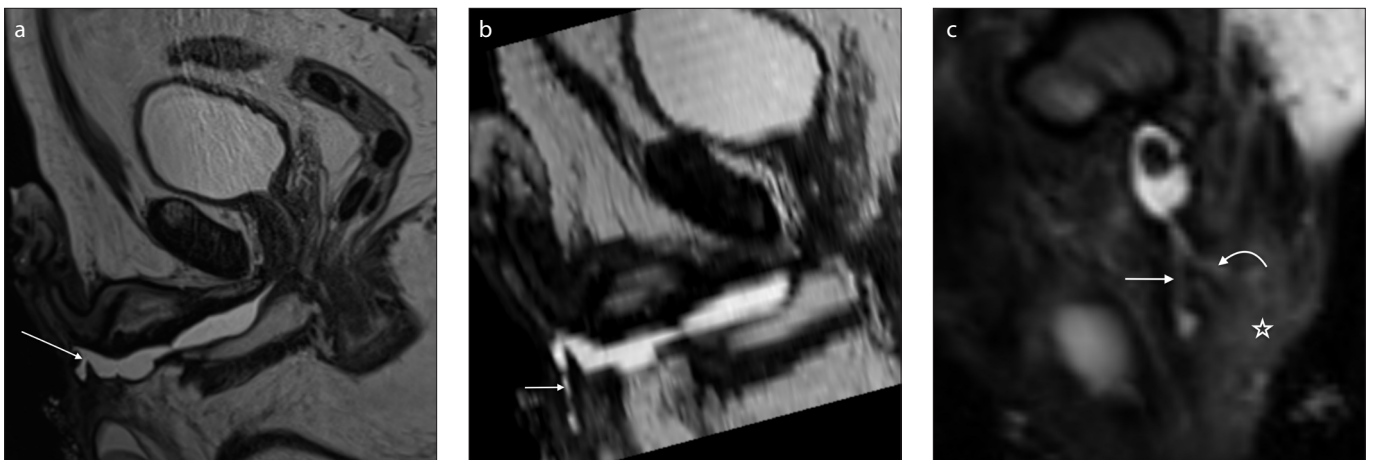


Figure 6. a–c. A 59-year-old patient with multiple stenoses of the urethra complicated by a branching urethrocutaneous fistula. T2-weighted sagittal image (a) shows the origin of the urethrocutaneous fistula (arrow). Parasagittal reformatted image (b) shows the main tract of the fistula (short arrow). Paracoronal reformatted image (c) shows a second branch of the fistula (curved arrow). Signs of inflammation of the adjacent soft tissue are also visible (asterisk).

MRU provided additional information in 2 patients with posterior urethra lesions. First patient was diagnosed with rectourethral fistula, while second patient had a posterior urethral disruption. Another patient was misdiagnosed by RUG, which showed a short stricture with proximal urethral diverticulum instead of a primary urethral tumor, properly diagnosed by MRU. MRU also enabled diagnosis of an accidental finding—a bladder tumor which was missed by VCUG. Some authors also described a technique of virtual cystoscopy using MRI that enables evaluation of the urethra and bladder wall. A virtual endoscopic view of the urethra is created on the basis of multiplanar images obtained in the MRI study. Authors compared these reconstructed images to conventional imaging methods revealing efficacy at a similar level (32, 36, 37). Moreover, due to more detailed data

on periurethral tissue provided by MRU, it may play a vital role in postoperative assessment of treatment effects, in particular in post-traumatic patients with posterior urethra stricture in whom the outcomes of surgical treatment are not satisfactory.

Discussion

Numerous treatment options have been developed and described for urethral stricture disease; however, decision is multifactorial with stricture location and length being the most critical of these factors. Conventional studies such as RUG and VCUG demonstrating luminal pathologies have been the gold standard diagnostic method for urethral strictures for nearly a century; however they are limited in imaging of the periurethral tissues. Preoperative assessment of the extent of spongiofibrosis is crucial for appropriate diagnosis and therapy and as such is required from radiologists (38). As a consequence, alternative imaging techniques, particularly SUG and MRU have been increasingly implemented in diagnostics algorithm, providing sufficient soft tissue contrast, depicting the urethra and periurethral tissues with the advantage of avoiding radiation.

Indications for application of MRU in patients with urethral stricture still remain to be specified. Restriction of MRU to patients who would benefit the most would prove cost-effective and limit its use. However, it is challenging to determine who would benefit the most due to the small number of clinical studies and lack of randomized trials. Based on the publications included in this review, MRU imaging seems to be the best imaging tool to assess post-traumatic pelvic anatomy (35). However, combined antegrade-retrograde urethrography remains the gold standard for preoperative assessment

of posterior urethral distraction defects (39). Usually, patients are assessed with RUG, followed by the VCUG frequently performed after filling the bladder with contrast medium via suprapubic catheter. However, in patients with diminished bladder volume after months of suprapubic diversion, filling the bladder may be painful and sometimes hardly possible. Thus, it is frequently impossible to evaluate the urethra during voluntary voiding. Under such circumstances, a curved metal sound can be transversed through the suprapubic cystostomy into the bladder. After placing the sound through the bladder neck, the proximal limit of the stricture may be detected. This procedure should always be performed by experienced urologists because of the risk of bladder damage, bleeding and severe pain (33). Another important limitation of VCUG results from difficulties with positioning the patient and possible underestimation of the length of the stricture when the axis of urethra is too horizontal or vertical (19). Urethral segment proximal to the stricture may not be depicted in RUG combined with VCUG. This may be overcome by MRU with T2-weighted and contrast-enhanced T1-weighted sequences enabling the imaging of the entire course of the urethra, prostate and periurethral structures with high accuracy. Several publications have reported significant changes of scheduled procedure, following the use of MRU preoperatively. Oh et al. (35) reported that MRI findings caused modification of surgical method in 11 of 25 patients after comparing the length of the stricture with VCUG results and assessment of spongiofibrosis. Similarly, Narumi et al. (40) stated that MRU findings altered the treatment method in 7 patients (26%) with stricture in the posterior part, Sung et al. (33) reported change

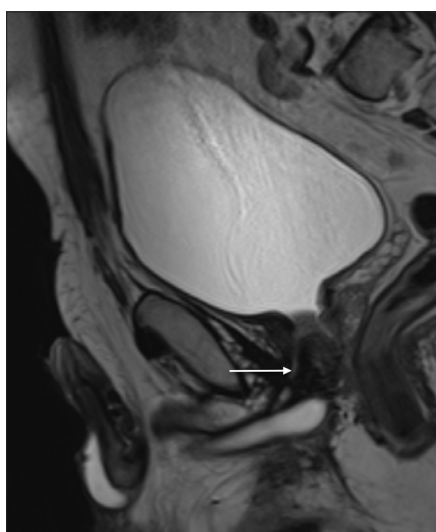


Figure 7. T2-weighted sagittal image shows presence of a false track (arrow) in a 59-year-old patient referred to our institution with suspicion of urethral stenosis.

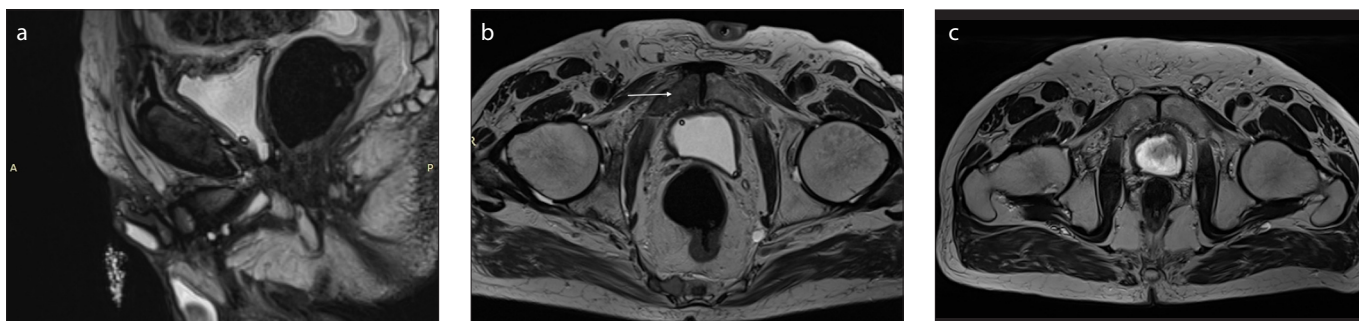


Figure 8. a–c. A 74-year-old patient who underwent radical prostatectomy was examined with MRI to evaluate urethral stricture associated with radiation therapy. T2-weighted sagittal (a) and axial (b) images show focal lesions within the minor pelvis bones (arrow) and lumbar spine suspected of being metastases, not present in a previous examination 10 months earlier as shown in T2-weighted axial image (c).

of the therapy in 7 of 10 patients (70%) with posterior urethral stricture, Osman et al. (30) in 4 patients (20%) with both anterior and posterior urethral strictures. Rastogi et al. (34) changed the surgical procedure in 1 patient (5%) with anterior urethral stricture. All authors emphasize the great advantage of MRU in assessment of periurethral pathologies and detailed reckoning of fibrosis with certain location and extent. Hence, MRU should be considered in patients in whom significant extent of spongiofibrosis is expected; for example, in patients after multiple optical urethrotomies or diagnosed due to post-traumatic urethral strictures. Compared with SUG, MRU overcomes the limitation of small field-of-view and significant subjectivity relative to the physicians' experience and skills.

In conclusion, MRU provides extra guidance for treatment planning including selection of optimal surgical procedure that cannot be obtained with standard diagnostic procedures. MRU should be taken into account in cases where standard methods do not give an unequivocal diagnosis or the operator has doubts about the choice of optimal surgical method. Based on the available literature, the greatest usefulness of MRU was demonstrated in post-traumatic urethral strictures, multiple strictures and long strictures with extensive spongiofibrosis. In most cases of patients with strictures located in the anterior urethra, the combination of RUG and SUG may deliver information comparable to MRU. However, MRU has the advantage of presenting more detailed data including possibility of acquiring three-dimensional reconstructions and showing concomitant pathologies without carrying risk of exposure to ionic radiation. Nonetheless, further studies on more numerous groups of patients should be designed and correlated with clinical outcomes in order to provide sufficient data on MRU indications and technique.

Conflict of interest disclosure

The authors declared no conflicts of interest.

References

- Jordan GH, Schlossberg SM. Surgery of the penis and urethra. In: Wein AJ, et al, eds. Campbell-Walsh Urology. Vol 1. 9th ed. Philadelphia, Pa: WB Saunders Co., 2007:1023–1097.
- Mundy AR. Management of urethral strictures. *Postgrad Med J* 2006; 82:489–499. [\[Crossref\]](#)
- Alwaal A, Blaschko SD, McAninch JW, Breyer BN. Epidemiology of urethral strictures. *Transl Androl Urol* 2014; 3:209–213.
- Baskin LS, Constantinescu SC, Howard PS. Biochemical characterization and quantitation of the collagenous components of urethral stricture tissue. *J Urol* 1993; 150:426–447. [\[Crossref\]](#)
- Wood DN, Andrich DE, Greenwell TJ, Mundy AR. Standing the test of time: The long-term results of urethroplasty. *World J Urol* 2006; 24:250–254. [\[Crossref\]](#)
- Almannie RM, Alkhamis WH, Alshabibi AI. Management of urethral strictures: A nationwide survey of urologists in the Kingdom of Saudi Arabia. *Urol Ann* 2018; 10:363–368. [\[Crossref\]](#)
- Maciejewski C, Rourke K. Imaging of urethral stricture disease. *Transl Androl Urol* 2015; 4:2–9.
- Peskar DB, Perović AV. Comparison of radiographic and sonographic urethrography for assessing urethral strictures. *Eur Radiol* 2004; 14:137–144. [\[Crossref\]](#)
- Bach P, Rourke K. Independently interpreted retrograde urethrography does not accurately diagnose and stage anterior urethral stricture: the importance of urologist-performed urethrography. *Urology* 2014; 83:1190–1193. [\[Crossref\]](#)
- Livingstone RS, Koshy CG, Raj DV. Evaluation of work practices and radiation dose during adult micturating cystourethrography examinations performed using a digital imaging system. *Br J Radiol* 2004; 77:927–930. [\[Crossref\]](#)
- McAninch JW, Laing FC, Jeffrey RB Jr. Sonourethrography in the evaluation of urethral strictures: a preliminary report. *J Urol* 1988; 139:294–297. [\[Crossref\]](#)
- Choudhary S, Singh P, Sundar E, Kumar S, Sahai A. A comparison of sonourethrography and retrograde urethrography in evaluation of anterior urethral strictures. *Clin Radiol* 2004; 59:736–742. [\[Crossref\]](#)
- Krukowski J, Kałużny A, Kłacz J, Matuszewski M. Comparison between cystourethrography and sonourethrography in preoperative diagnostic management of patients with anterior urethral strictures. *Med Ultrason* 2018; 20:436–440. [\[Crossref\]](#)
- Koraitim MM, Reda IS. Role of magnetic resonance imaging in assessment of posterior urethral distraction defects. *Urology* 2007; 70:403–406. [\[Crossref\]](#)
- Pandian RM, John NT, Eapen A, Antonisamy B, Devasia A, Kekre N. Does MRI help in the pre-operative evaluation of pelvic fracture urethral distraction defect? - a pilot study. 2017; 43:127–33. [\[Crossref\]](#)
- Moher D, Liberati A, Tetzlaff J, Altman DG, The PRISMA Group. (2009). Preferred reporting items for systematic reviews and meta-analyses: The PRISMA statement. *PLoS Med* 2009; 6:e1000097. [\[Crossref\]](#)
- Moher D, Shamseer L, Clarke M, et al. Preferred reporting items for systematic review and meta-analysis protocols (PRISMA-P) 2015 statement. *Syst Rev* 2015; 4:1–9. [\[Crossref\]](#)
- Ryu J, Kim B. MR imaging of the male and female urethra. *Radiographics* 2001; 21:1169–1185. [\[Crossref\]](#)
- Kawashima A, Sandler CM, Wasserman NF, LeRoy AJ, King BF, Goldman SM. Imaging of urethral disease: a pictorial review. *Radiographics* 2004; 24 (Suppl 1):S195–S216. [\[Crossref\]](#)
- Markiet K, Frankiewicz M, Belka M, Kozak O, Matuszewski M, Szurowska E. Magnetic resonance imaging in urethral strictures with a special focus on spongiofibrosis - from image to a 3D-print. Joint radiological and urological perspective. ECR 2018 Educational Exhibit. [\[Crossref\]](#)
- Altun E. MR imaging of the penis and urethra. *Magn Reson Imaging Clin N Am* 2019; 27:139–150. [\[Crossref\]](#)
- El-ghar MA, Osman Y, Elbaz E, Refaie H, El-Diasty T. MR urethrogram versus combined retrograde urethrogram and sonourethrography in diagnosis of urethral stricture. *Eur J Radiol* 2010; 74:e193–198. [\[Crossref\]](#)
- Park BK, Kim CK, Lee SW. Evaluation of anterior urethral stricture using thick slab SSFSE MR urethrography. *Acta Radiol* 2010; 51:1157–62. [\[Crossref\]](#)
- Pavlica P, Menchi I, Barozzi L. New imaging of the anterior male urethra. *Abdom Imaging* 2003; 28:180–186. [\[Crossref\]](#)
- Hanna SAZ, Abdel Rahman SF, Altamimi BA, Shoman AM. Role of MR urethrography in assessment of urethral lesions. *Egypt J Radiol Nucl Med* 2015; 46:499–505. [\[Crossref\]](#)
- Kim B, Kawashima A, LeRoy AJ. Imaging of the male urethra. *Semin Ultrasound CT MRI* 2007; 28:258–273. [\[Crossref\]](#)
- Del Gaizo A, Silva AC, Lam-Himlin DM, Allen BC, Leyendecker J, Kawashima A. Magnetic resonance imaging of solid urethral and peri-urethral lesions. *Insights Imaging* 2013; 4:461–469. [\[Crossref\]](#)
- Song L, Xie M, Zhang Y, Xu Y. Imaging techniques for the diagnosis of male traumatic urethral strictures. *J Xray Sci Technol* 2013; 21:111–123. [\[Crossref\]](#)
- Khalaf T, El-bab F, Mohamad E, Mohamad A, Farghally M. Magnetic resonance urethrography versus conventional retrograde urethrography in the evaluation of urethral stricture: Comparison with surgical findings. *Egypt Soc Radiol Nucl Med* 2015; 46:199–204. [\[Crossref\]](#)
- Osman Y, El-Ghar MA, Mansour O, Refaie H, El-Diasty T. Magnetic resonance urethrography in comparison to retrograde urethrography in diagnosis of male urethral strictures: is it clinically relevant? *Eur Urol* 2006; 50:587–594. [\[Crossref\]](#)
- Contrast Media Safety Committee ESUR. Guidelines on Contrast Media v10. CMSC, 2018. Available at: <http://www.esur-cm.org/index.php/>
- Yekeler E, Suleyman E, Tunaci A, et al. Contrast-enhanced 3D MR voiding urethrography: Preliminary results. *Magn Reson Imaging* 2004; 22:1193–1199. [\[Crossref\]](#)
- Sung DJ, Kim YH, Cho SB, et al. Obliterative urethral stricture: MR urethrography versus conventional retrograde urethrography with voiding cystourethrography. *Radiology* 2006; 240:842–848. [\[Crossref\]](#)
- Rastogi R, Joon P, Pushkarna A, et al. Comparative role of sonourethrography (SUG) and magnetic resonance urethrography (MRU) in anterior male urethral strictures. *Ann Clin Lab Res* 2016; 4:1–4. [\[Crossref\]](#)
- Oh MM, Jin MH, Sung DJ, Yoon DK, Kim JJ, Moon DG. Magnetic resonance urethrography to assess obliterative posterior urethral stricture: comparison to conventional retrograde urethrography with voiding cystourethrography. *J Urol* 2010; 183:603–607. [\[Crossref\]](#)
- Suleyman E, Yekeler E, Dursun M, et al. Bladder tumors: Virtual MR cystoscopy. *Abdom Imaging* 2006; 31:483–489. [\[Crossref\]](#)

37. Bernhardt TM, Rapp-Bernhardt U. Invited update: Virtual cystoscopy of the bladder based on CT and MRI data. *Abdom Imaging* 2001; 26:325–332. [\[Crossref\]](#)
38. McAninch JW, Laing FC, Jeffrey RB. Sonourethrography in the evaluation of urethral strictures: A preliminary report. *J Urol* 1988; 139:294–297. [\[Crossref\]](#)
39. Gelman J, Wisenbaugh ES. Posterior urethral strictures. *Adv Urol* 2015; 2015:628107. [\[Crossref\]](#)
40. Narumi Y, Hricak H, Armenakas NA, Dixon CM, McAninch JW. MR imaging of traumatic posterior urethral injury. *Radiology* 1993; 188:439–443. [\[Crossref\]](#)